

Generative Design for Self-balancing Unicycle Robot in Additive Manufacturing

Jiaqi Chen[†]

School of Mechanical Engineering
Tongji University
Shanghai China
1753786@tongji.edu.cn

Qilong Cheng

Faculty of Applied Science and
Engineering
The University of Toronto
Toronto ON Canada
qilong.cheng@mail.utoronto.ca

Mengrui Han

Faculty of Materials and
Manufacturing
Beijing University of Technology
Beijing China
hanmengrui@emails.bjut.edu.cn

Corresponding Author*: Jiaqi Chen (e-mail: 1753786@tongji.edu.cn) d
These authors contributed equally.

ABSTRACT

Chassis structures have a fundamental influence on the stability of self-balancing unicycles. This paper documents how using generative design can improve the robotic system's stability and reduce the overall mass compared to the conventional designs. The chassis structure is divided into seven parts for stress analysis. According to the results from the stress analysis, loading conditions and constraints can be set for the generative studies. The ideal solutions were chosen based on the mass-safety factor graphs for the most optimized geometry. Stress analysis was then carried out on Inventor to verify the model's reliability. To test the controllability of the generative unicycle, simulations were carried out in Simulink by comparing the generative design with the conventional design. The results showed that the generative chassis structure has a higher center of mass and lower mass, hence is easier to achieve balancing from an angular deviation.

KEYWORDS

generative design; structural topology optimization; bi-directional evolutionary optimization; unicycle robot; dynamic system control

1 Introduction and Background

Generative design is an iterative process involving an artificial intelligence algorithm that generates solutions based on the design constraints by mimicking natural selections. This design process breaks the traditional design methods. Instead of setting each parametric dimension, the designer or engineer inputs design goals into the generative design software, along with parameters such as performance or spatial requirements, materials, manufacturing methods, and cost constraints [1]. The designer or engineer will then fine-tune the feasible designs by

changing the input parameters and selecting the most optimized solution.

The generative design process is widely used for aerospace, constructions, and even interior designs [2]. For instance, Czinger 21C implemented this technology and revolutionized formula racing cars by using AI to design the whole car [3]. The resulting vehicle can achieve a stunning 0-62mpr in only 1.9 seconds. Airbus also formed a team called "the bionic partition" to design an unassuming but critical piece of the aircraft: the partition that separates the passenger compartment from the galley in the Airbus A320 cabin. The results are significantly lighter than the existing ones with the same structural rigidity and functions. Keep in mind that 1kg of weight reduction is 106kg of jet fuel saved up each year; this is hugely beneficial to environmental protection [4]. Additionally, generative designs can be incorporated into contemporary product designs to create Voronoi patterns, procedural networks, and generative structures for aesthetic and function purposes [5]. Multiple studies on topology optimizations have also been done to optimize the weight of robotic arms. Those studies are mostly related to finite element analysis on the structural design. Designers can then model the optimized model based on the topology optimized results to get an ideal design [6]. Dinh Son Nguyen [7] proposed topological optimization as additive manufacturing (3D printing) design method to help designers create optimal product structures with the least materials on the premise of ensuring the mechanical properties of products. Additive manufacturing requires no process planning and can be manufactured for any complex shape without being limited by the manufacturability of the material. This paper presents a novel method of using topology optimization as an innovative design tool, which can provide ideas for additive manufacturing design and help users complete the design with the lowest cost under the premise of guaranteeing the original performance. Gao Yongxin [8] combined advanced materials with advanced

manufacturing technology. Combined with the topology optimization technology, the topology optimization design of the small satellite star tracker support was carried out, and then the model of the star tracker support was redefined by additive manufacturing technology. In the end, the weight of the star tracker was significantly reduced compared to the pre-optimization while maintaining the required stiffness and strength.

In robotics, mass is critically related to the efficiency of a robotic system. Having a lightweight but rigid structure can drastically increase the accuracy of robotic arms and mobile robots' path following capability [9]. Hence, instead of using the traditional human design method, we decided to implement a generative design from Fusion 360 by Autodesk to reduce our robot's weight. Our research will study how optimized structural design will benefit the robots' responsiveness and controllability. Specifically, a self-balancing unicycle robot is chosen as our testing subject. Studies have done on this using a reaction wheel and bottom wheel to keep the pitch and roll angles in equilibrium states [10]. However, the overall structure of the robots is mostly unoptimized, causing control difficulty and excessive use of energy.

The responsiveness and controllability can be easily reflected via the time it takes for the unicycle to return to the equilibrium vertical position when there is a deviation from vertical orientation at the initial position. This paper will document the detailed generative design process and the math behind each part's loading conditions. Then the generated unicycle model will be compared to the traditionally made unicycle in Simulink based on the control system settling time, peak value, and power consumption.

2 Structural Design and Analysis

First, during preparation, a simple model of the unicycle is created for dimensional reference and later, the generative design process. And the unicycle is divided into several crucial components based on the loading conditions to minimize cloud compute costs. (As seen in Fig. 1)

Step 1: identify force distributions and draw the free-body diagrams for each component.

In total, seven parts are created separately and then will be merged as one piece for 3D printing. Each part will go through the same generative design process as listed below:

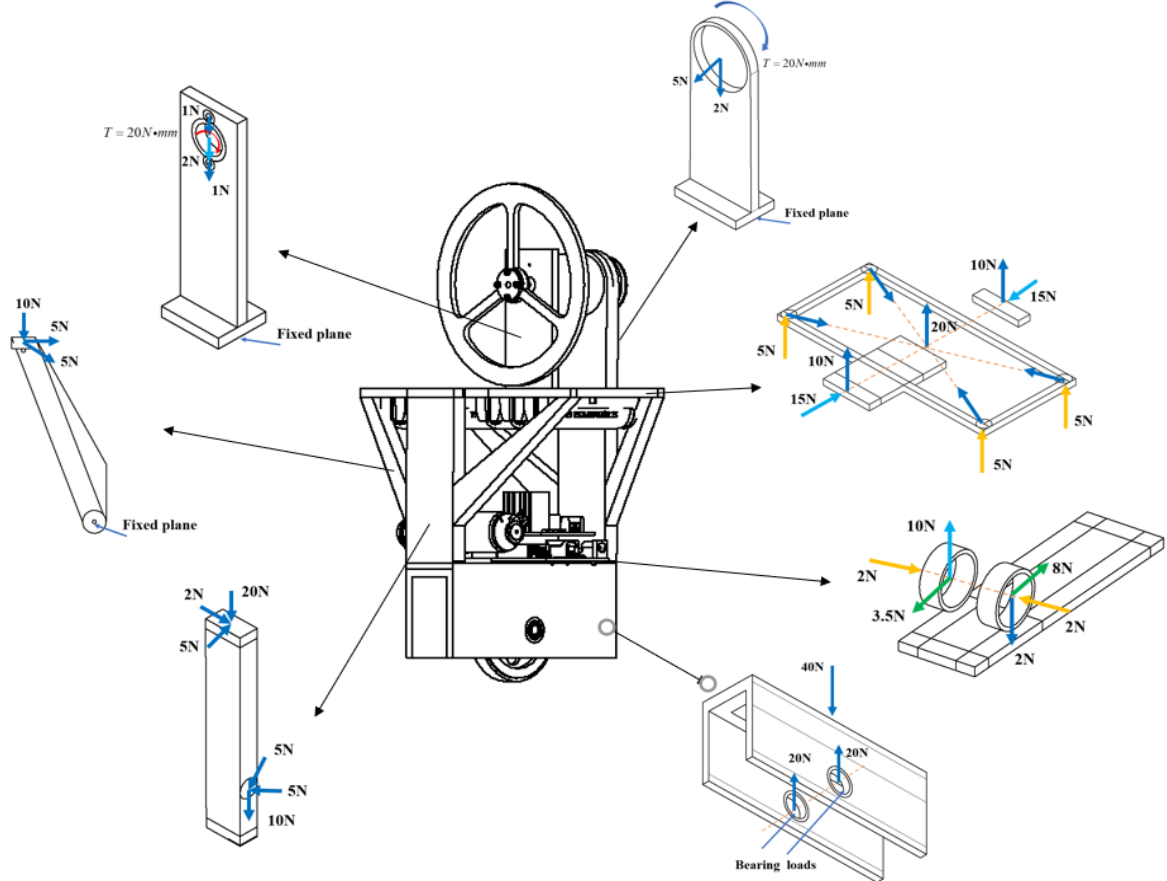


Figure 1: Stress analysis on each component of the unicycle body

Table 1. Mass of each component in a unicycle

Name	Mass
Reaction Wheel and its Motor	165.6g + 74.32g
Bottom Motor	96g
Batteries	135g
Electrical Components	10g
Entire Body Weight Estimate	169.03g

Before starting the generative process, an approximate theoretical force distribution analysis is done based on the mass for the physical components the structure needs to support. The unicycle comprises five central units: the bottom drive wheel,

drivetrain system, reaction wheel, attached motor, batteries, and electrical components. The designed safety factor during experiments is set as 2 to have a longer service life.

Step 2: design the reserves and obstacles for designed parts, and set starting shape if necessary.

This design process will be done entirely in the Fusion 360 Generative Design workspace following the force analysis done in step one. Since the unicycle body is a complex system in both static loading conditions and dynamic loading conditions, seven parts are divided to make up the whole-body structure. Ones shown in green are the preserved parts for joints and grounds which will be kept during generative studies; red represents the obstacles where no materials will be generated, and yellow is the starting shape for the generative design to take place. The starting shape is optional but can save up processing times for our studies. Grey ones are the conventional design and can be considered as a reference to understand a component's shape.

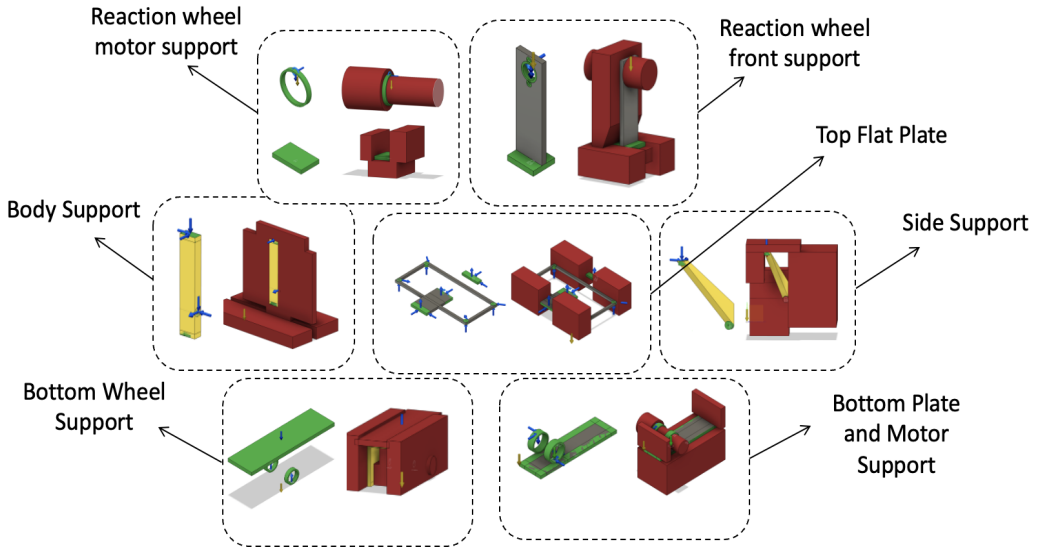


Figure 2: Input constraints and loading conditions on the generative design workspace

Step 3: constrain the materials selection and manufacturing methods.

In order to generate a wide range of possible solutions, no constraints are set for manufacturing methods. Since all components generated will be made via liquid 3D printing, Nylon, ABS plastics, Acrylic, Resin, Aluminum and Titanium are chosen for most generated parts. However, our research only allows budgets for Nylon 3D printing. Hence, only Nylon considered in the scope during the final selection.

Step 4: generating desired solutions and processing simulation for validation and selection

After defining all parameters and inputs from steps 2 and 3, solutions can be computed via the Fusion 360 cloud service. Figure 3 illustrates a number of possible solutions for the study, and Figure 4 displays a graphical relationship between mass and safety factor of different materials. In the graph, the thumb symbols showcase the ideal solution computed by the computer based on all the inputs and goals we set in steps 2 and 3. Final solutions are chosen as the closest Nylon material solution near the thumbed symbol



Figure 3. Generative design materials subtraction process

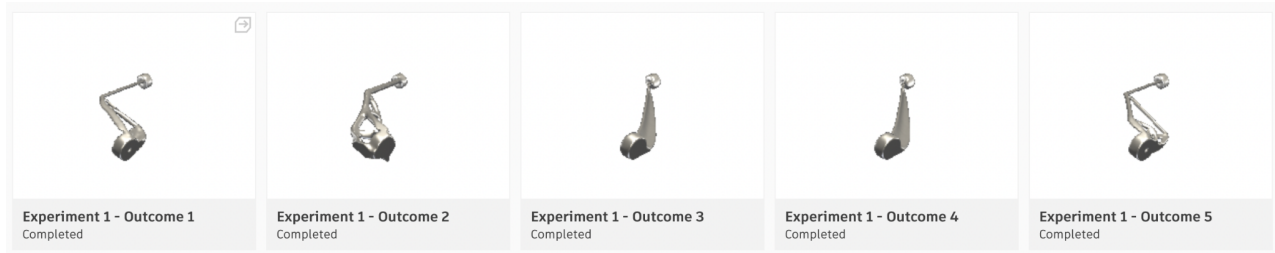


Figure 4. Generative design solution examples

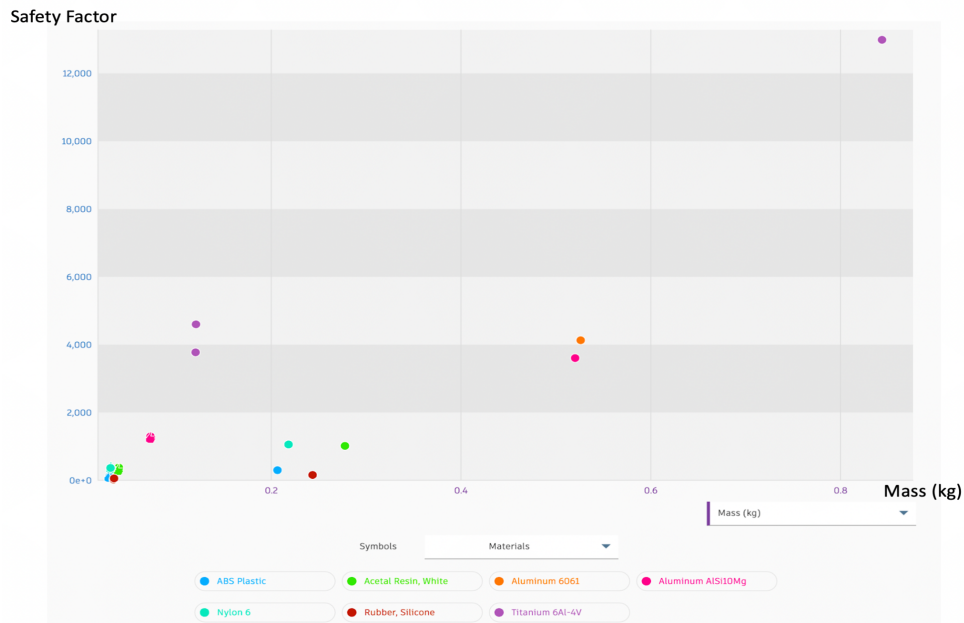


Figure 5. Safety factor - Mass comparison between solutions

Step 5: post-processing the optimal solution

Since the moment analysis only considers force on one single side, mirroring of the generated body is needed to achieve the final result. An example can be seen below where two mirror actions took place to achieve the same rigidity in all four bending directions.

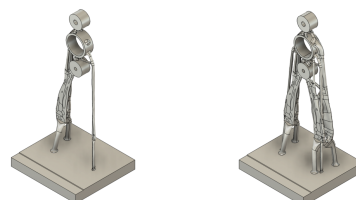


Figure 6: Post-processing mirroring result example

Additionally, during research, we found that over-constrained models will generate undesired solutions. When defining an excessive amount of preserved parts, the generated parts will be too minimal to have a drastic mass reduction. An example is given on the difference between over constrained and minimally constrained solutions:



Figure 7: Comparison between over-constrained solution and solution with little constraints

Based on the force distribution mentioned in the Structural design and analysis, stress analysis on the structure is performed in Inventor. By using finite element analysis, relevant loads and constraints are set to perform the stress analysis. The result of the stress analysis is shown in the figure below.

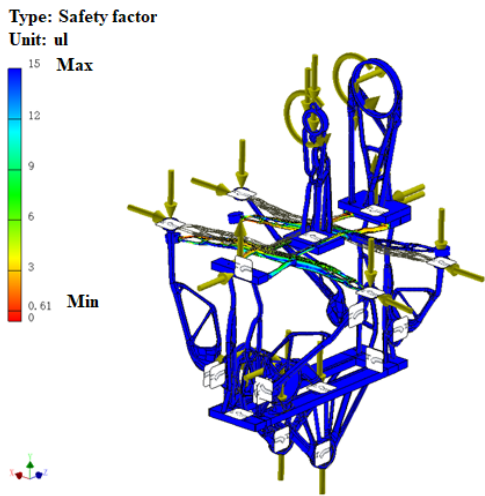


Figure 8: Safety factor

The safety factor is greater than 15, which means that it can safely bear the applied load and meet the design requirements.

Finally, once each component is generated and tuned for post-processing, a full assembly can be obtained and 3D printed as one single piece.

3 Kinetics Simulation Analysis

For every achievable system, simulation is the essential part before actually commencing the building process of real parts. To break down the core structure of the self-balancing unicycle, we analyze the main methods of balancing used widely today. The first one is a reaction wheel, which we have already decided to use. The second one is to use the motor to offer a torque to offset the collapse torque by the inertial force. In our model,

because we have to control the balance in two directions (roll and pitch), we can use both methods to achieve our goal.

Also, there is another DOF that needs to be controlled. The translation motion along the direction of the bottom wheel needs to be restricted since the unicycle will certainly move arbitrarily otherwise.

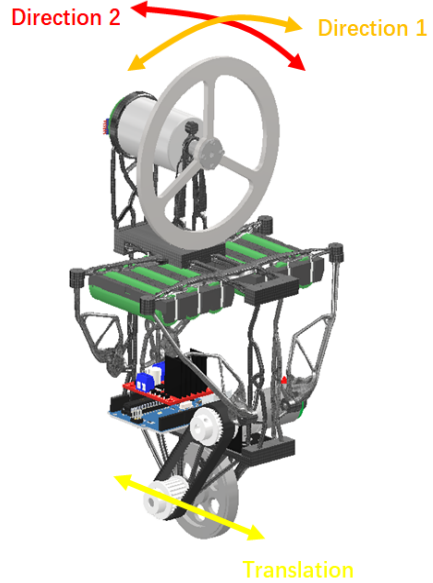


Figure 9: Demonstration of DOFs

To give the motion a more accurate understanding, a set of mathematical equations can be built as follows:

First, analyzing the system based on the brushed DC motor analysis, we can derive the input torque matrix and the angular output matrix:

$$\mathbf{q} = \begin{bmatrix} \theta_2 \\ \phi \\ \theta_1 \\ \varphi \end{bmatrix}, \boldsymbol{\tau} = \begin{bmatrix} \tau_2 \\ -\tau_2 \\ \tau_1 \\ -\tau_1 \end{bmatrix} \quad (3.1)$$

Namely, θ_2 is the reaction wheel rotational angle, θ_1 is the bottom wheel rotational angle, φ is the pitch angle, ϕ and θ_1 is the roll angle. τ_1 and τ_2 represent torque provided by the reaction wheel and the bottom wheel, respectively.

The torque and angular relationship can be found as:

$$\frac{d}{dt} \frac{\partial L}{\partial \dot{\mathbf{q}}} - \frac{\partial L}{\partial \mathbf{q}} = \boldsymbol{\tau} \quad (3.2)$$

Where L is the total lagrangian, \mathbf{q} is the rotational angle matrix, and $\boldsymbol{\tau}$ is the torque matrix provided by the system.

Then, based on the Lagrange mechanics, the system can be interpreted as potential energy dividing kinetic energy.

$$L = E - U \quad (3.3)$$

Where the kinetic energy is:

$$E = \frac{1}{2} J_{ty} \dot{\varphi}^2 + \frac{1}{2} J_{tx} \dot{\phi}^2 + \frac{1}{2} J_1 \dot{\theta}_1^2 + \frac{1}{2} J_2 \dot{\theta}_2^2 \quad (3.4)$$

J_{ty} J_{tx} represents the mass moment of inertia of the system over the x and y axis, and J_1 J_2 represent the mass moment of inertia of the bottom wheel and reaction wheel.

And potential energy is:

$$U = M_t \cdot g \cdot l_b (\cos \varphi \cdot \cos \phi) \quad (3.5)$$

M_t is the system's total mass, l_b is the distance between the system's center of gravity to the ground contact point.

Substitute both equations (3.4) and (3.5) into (3.2), we can obtain:

$$J_2 \ddot{\theta}_2 + \frac{K_{E_2} K_{T_2} \cdot 60}{2\pi R_{S_2}} \dot{\theta}_2 = \frac{K_{T_2} U_{dr2}}{2R_{S_2}} \quad (3.6)$$

$$J_{tx} \ddot{\phi} - M_t g l_b \sin \varphi \cos \phi - \frac{K_{E_2} K_{T_2} \cdot 60}{2\pi R_{S_2}} \dot{\theta}_2 = -\frac{K_{T_2} U_{dr2}}{2R_{S_2}} \quad (3.7)$$

$$J_1 \ddot{\theta}_1 + \frac{K_{E_1} K_{T_1} \cdot 60}{2\pi R_{S_1}} \dot{\theta}_1 = \frac{K_{T_1} U_{dr1}}{2R_{S_1}} \quad (3.8)$$

$$J_{ty} \ddot{\phi} - M_t g l_b \sin \varphi \cos \phi - \frac{K_{E_1} K_{T_1} \cdot 60}{2\pi R_{S_1}} \dot{\theta}_1 = -\frac{K_{T_1} U_{dr1}}{2R_{S_1}} \quad (3.9)$$

K_{T_1} , K_{T_2} , K_{E_1} , K_{E_2} are the bottom wheel motor torque constant, bottom wheel motor electrical constant; reactionary wheel motor torque constant, and reaction wheel motor electrical constant respectively. R_{S_1} and R_{S_2} are the bottom wheel's motor resistance and the reaction wheel's motor resistance. Rearrange equations (3.6) ~ (3.9), we can get the matrix form:

$$\mathbf{M} \cdot \ddot{\mathbf{q}} + \mathbf{V}(\mathbf{q}, \dot{\mathbf{q}}) = \mathbf{p} \cdot \mathbf{u} \quad (3.10)$$

Where:

$$\mathbf{u} = [u_{dr1}, u_{dr2}]' \quad (3.11)$$

$$\mathbf{M} = \begin{bmatrix} J_1 & 0 & 0 & 0 \\ 0 & J_{tx} & 0 & 0 \\ 0 & 0 & J_2 & 0 \\ 0 & 0 & 0 & J_{ty} \end{bmatrix} \quad (3.12)$$

$$\mathbf{p} = \begin{bmatrix} \frac{K_{T_2} U_{dr2}}{2R_{S_2}} & 0 \\ -\frac{K_{T_2} U_{dr2}}{2R_{S_2}} & \frac{K_{T_1} U_{dr1}}{2R_{S_1}} \\ 0 & -\frac{K_{T_1} U_{dr1}}{2R_{S_1}} \end{bmatrix} \quad (3.13)$$

$$\mathbf{V} = \begin{bmatrix} \frac{K_{E_2} K_{T_2} \cdot 60}{2\pi R_{S_2}} \dot{\theta}_2 \\ -M_t g l_b \sin \varphi \cos \phi - \frac{K_{E_2} K_{T_2} \cdot 60}{2\pi R_{S_2}} \dot{\theta}_2 \\ \frac{K_{E_1} K_{T_1} \cdot 60}{2\pi R_{S_1}} \dot{\theta}_1 \\ -M_t g l_b \sin \varphi \cos \phi - \frac{K_{E_1} K_{T_1} \cdot 60}{2\pi R_{S_1}} \dot{\theta}_1 \end{bmatrix} \quad (3.14)$$

Additionally, the block diagram below clearly shows the control method. To simplify the understanding of the combined effect of various DOFs, we can see the translation together with the pitch rotation as the motion of an inverted pendulum and the roll direction as a separated part. The control method uses PID controllers.

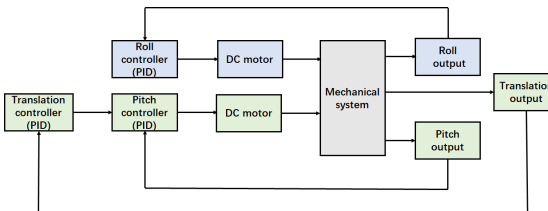


Figure 10: Control system diagram

To simulate this process, we choose the Simulink with Simscape to establish the kinetics model of the unicycle. Simscape provides a direct way to simulate a complex nonlinear system. Using a wide range of modules, we built the system model as follows:

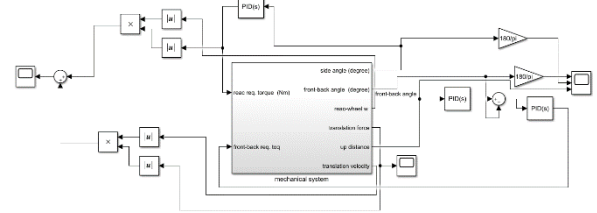


Figure 11: the control layer of Simulink diagram

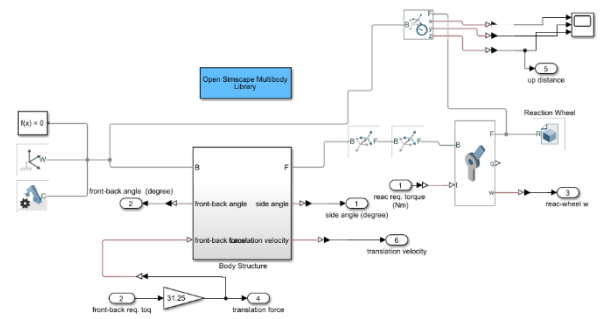


Figure 12: the general mechanical layer of Simulink diagram

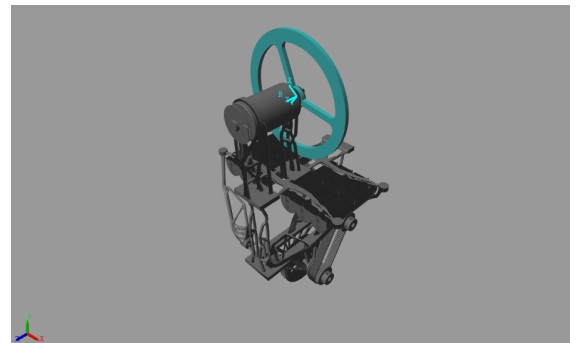


Figure 13: Simulation in process

In the PID controllers, we use the requested torque as the output to the DC motors and the motion parameters from the sensing modules as the input. There are three PID blocks altogether, which control the roll, pitch axis, and translation motion. The same set of PID parameters are used to give an identical test environment to provide a convincing comparison between the model after generative design and the conventional one.

After importing the two models and running the simulation, we get the following results with an initial value (5 degrees) for both rotational axes.

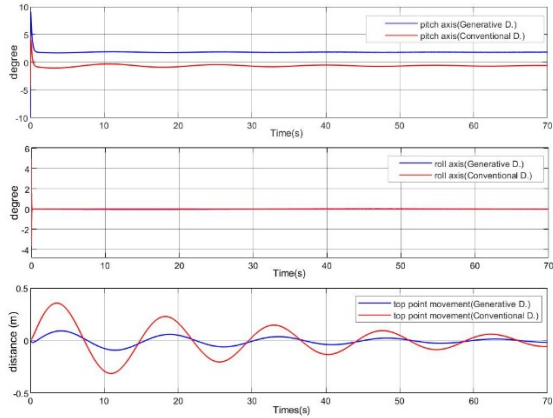


Figure 14: Simulation results

Table 2. Analysis of Simulation results

	Settling time Gene.	Settling time Conv.
pitch	0.6876s	19.2123s
roll	0.0598s	0.06s
	Peak time Gene.	Peak time Conv.
	4.1729s	3.5946s
Top point movement	Peak value	Peak value
	0.092m	0.3562m
Power consumption reference	Gene.	Conv.
P_{mean}	3.401×10^2	3.475×10^2
P_{max}	2.759×10^6	2.984×10^6
t_{max}	$1.3 \times 10^{-3}s$	$1.4 \times 10^{-3}s$

It is evident that the improved structure with a higher center of mass from the generative design made the unicycle easier to maintain its balance. In the 70-second simulation, the unicycle achieved a significant decrease in the average amplitude of the top point movement, which describes the movement of the highest point on the total unicycle. As for the results in the roll axis, it is almost identical. As for the results in the pitch axis, the error is inevitable and has a varying value for each because

the PID parameter set is fixed and not tailored for every different structure. Thus, a long-term deviation from the zero point must exist. In addition, if we closely observe the results, we may notice that the conventional design result has a small but more noticeable fluctuation than the generative one. It results in a significantly prolonged settling time of the conventional unicycle. (The settling time was measured based on a range of 5% of the difference between the initial error and the final value. If the initial value is seen as the origin, the mentioned difference can be considered as a step signal with a given height equal to that difference. Thus we can use the settling time to evaluate the simulation results.) This also demonstrates the advantage of the generative design structure.

Also, we have estimated the power consumption of both structures. We calculated the consumption value based on the two DC motors. Because the simulation was run under an ideal condition, the results we got should be seen as reference values. From the average power consumption perspective, the generative design can save about 2.13% energy during the 70s simulation in comparison with the conventional one. The peak power of the generative design appeared not only lower but also sooner. This corresponds with the results from the settling time comparison.

4 Conclusion

In this paper, a structural improvement based on generative design has been proposed and tested on a self-balancing unicycle using PID controllers. After the stress analysis according to the loading condition, the whole structure went through a generative design process. Then, by setting an initial position error, the generative version has been compared with the conventional one in Simulink under identical conditions. From the perspectives of responding evaluation and energy consumption, we conclude that the unicycle based on generative design generally possesses a better ability to return to equilibrium.

5 Outlook

The simulation method we used has its limitations. In our mathematical models as well as in the Simulink section, we didn't consider the effect of friction. The Fluctuation in the results may be significantly damped with the existence of friction. In our future work, we will take that factor into consideration and build real models using Nylon 3D printing to deliver a more cogent comparison.

ACKNOWLEDGEMENTS

The authors are grateful to the professors and teachers who gave constructive comments and advice during the whole period of the research project. They helped make the content more innovative and present the results in a concise and clear way.

REFERENCES

- [1] Autodesk.com, What is Generative Design | Tools Software | Autodesk, <https://www.autodesk.com/solutions/generative-design>.
- [2] Sun Hongbo and Ling Ma (2020). Generative Design by Using Exploration Approaches of Reinforcement Learning in Density-Based Structural Topology Optimization. *Designs*, 4(2), 10.
- [3] Czinger K, Czinger, <https://www.czinger.com/about-21-c>.
- [4] Autodesk.com, Generative Design at Airbus | Customer Stories | Autodesk, <https://www.autodesk.com/customer-stories/airbus>.
- [5] Lobos A (2018). Finding balance in generative product design.
- [6] Sha Liansen, Andi Lin, Xinqiao Zhao and Shaolong Kuang (2020). A topology optimization method of robot lightweight design based on the finite element model of assembly and its applications. *Science Progress*, 103(3), 0036850420936482.
- [7] Nguyen DS, Vignat F (2018). Topology optimization as an innovative design method for additive manufacturing. 2017 IEEE International Conference on Industrial Engineering and Engineering Management (IEEM), 304-308.
- [8] Gao Y, Zhang L and Liu Z (2019). Optimization Design of Star Tracker Bracket of Small Satellite for 3D Printing. 2019 5th International Conference on Control, Automation and Robotics (ICCAR), 808-811.
- [9] Ye Dongsen, Shaoming Sun, Jian Jhen Chen and Minzhou Luo (2014). The lightweight design of the humanoid robot frameworks based on evolutionary structural optimization. 2014 IEEE International Conference on Robotics and Biomimetics (ROBIO 2014), 2286-2291.
- [10] Neves and Gabriel P (2017). Modeling, construction and control of a self-balancing unicycle. Doctoral dissertation, Universidade de São Paulo.